Multi-Objective Optimization of Energy Storage Siting and Sizing Problem

Md Shamim Hasan[1], Willie Aboumrad[2], Phani R. V. Marthi[1], and Suman Debnath[1]
Power System Resilience, Oak Ridge National Laboratory, Oak Ridge, TN, 37932, USA[1]
IonQ Inc., College Park, Maryland, USA[2]
Email: hasanm1@ornl.gov, aboumrad@ionq.co, marthip@ornl.gov, and debnaths@ornl.gov

***Abstract*— Extensive integration of power electronics-based systems has transformed modern power networks significantly, yet their inherent variability and intermittency pose significant challenges to grid stability and reliability. Energy Storage Systems (ESS) offer a promising solution by rapid sharing capabilities that enhance voltage regulation, system stability, and overall reliability. To fully use the benefits of ESS, strategic decisions regarding their optimal placement and sizing are essential. While prior research has addressed aspects of this problem, integrated frameworks that simultaneously minimize voltage deviation, reduce power flow deviation from substations, and account for installation and operational energy costs remain limited. In addition, solving the combined siting and sizing problem is computationally challenging because binary siting decisions yield a mixed-integer optimization model; such combinatorial formulations are NP-hard in general and become increasingly computationally expensive to solve at scale. Hence, this paper presents a comprehensive two-stage methodology for determining the optimal siting and sizing of ESS where siting problem is separated from the classical optimization problem to reduce the scalability and computational challenges. In addition, the paper investigates the comparison of solutions and their impacts between non-linear, quadratic, and convex formulations.**

***Index Terms*—Energy Storage System (ESS) Optimal Placement and Optimal Sizing, Energy Storage Cost, Convex Relaxation, Non-linear Optimization, Quadratic Programming.**

I. Introduction

The growing integration of power electronics-based systems (PESs) into distribution networks presents significant operational challenges, such as, management challenges, voltage limit violations, increased system losses, and reduced system resilience [1]. Energy Storage Systems (ESS), with their ability to regulate power and swift transition over time, may play an important role in addressing these issues. They help accommodate fluctuating PES output, reduce the effect of load variations, and improve voltage stability across the network [1]. However, the effectiveness of ESS in supporting grid operations and enhancing PES integration is highly dependent on their placement and sizing. Strategically allocating ESS can minimize investment costs [2], ensure optimal performance, and yield system-wide benefits [3]. A comprehensive approach to ESS sizing and siting that addresses multiple operational objectives simultaneously is essential for comprehensive network improvement.

Extensive research has been conducted on determining the optimal location and sizing of ESS in distribution networks to address key challenges associated with PESs, such as intermittency, voltage deviations, and cost efficiency. ESS has demonstrated its effectiveness in mitigating these issues and enhancing overall system performance [4]. Firstly, ESS can store excess electricity generated by PESs and release it when needed, improving supply stability and enabling efficient load management [5]. Secondly, it helps with time-shifting: energy produced during the day can be used to meet demand later at night, which enhances the self-consumption rate of energy and helps to reduce overall electricity costs [6]. In addition, ESSs offer additional benefits including operational independence, rapid response to demand fluctuations, improved long-term energy management, enhanced reliability of electricity supply, and uninterrupted power delivery [7].

One of the early studies on optimal sizing and placement of ESS is presented in [8] where the minimum required capacity and optimal location is determined by optimizing the exchange of both active and reactive power between the ESS and its grid-tied inverter (GTI), taking into account the network topology and the system's R/X ratios. However, the approach may face scalability challenges due to the required inversion of the equivalent impedance matrix ($Z_{eq_{kj}}$). Convex optimization was applied in [9] to find the optimal size of ESS in an off-grid microgrid, aiming to minimize total costs including fuel, installation, operation, and maintenance. ESS sizing optimization was presented in [10], focusing on reactive power support and voltage profile improvement in a 36-bus system using Genetic Algorithm (GA). In addition, [11] employed the Grasshopper Optimization (GO) method to optimize ESS capacity and placement, reducing line loss and voltage profile improvement.

Several studies have adopted multi-objective optimization approaches to determine the optimal placement and sizing of ESS. In [7], a multi-objective framework was proposed for shared ESS deployment in urban energy communities, aiming to balance economic, technical, and environmental performance by minimizing the net present value of installation and maximizing energy self-efficiency. However, this work did not address voltage deviation. The study in [12] considered minimizing total costs and voltage deviations, but did not look into substation power flow deviation. In [13], a multi-objective model was developed to minimize bus voltage fluctuation, energy storage capacity, and substation power deviation with a 24-hours 24-steps problem, but it did not consider system cost. These studies employed heuristic algorithms, such as, GA, Peafowl Optimization Algorithm, and Particle Swarm Optimization to solve their respective optimization problems. While heuristics are flexible and widely used, they are typically problem-specific, computationally expensive, and fail to achieve global optimality [14]. In contrast, convex and quadratic optimization methods are generally preferred for their well defined mathematical structure, superior convergence properties, and scalability across larger systems.

Based on the preceding discussion, it is evident that existing research lacks a comprehensive approach to the optimal sizing and placement of ESS that simultaneously considers cost minimization, reduction of voltage deviation, and substation power flow minimization. Furthermore, limited studies have explored the comparative performance of quadratic and convex

This work was supported by the U.S. Department of Energys' Grid Modernization Initiative (GMI) Grid Research, Integration, and Deployment for Quantum (GRID-Q) project. This manuscript has been authored by UT-Battelle, LLC under Contract No. DE-AC05-00OR22725 with the U.S. Department of Energy. The United States Government retains and the publisher, by accepting the article for publication, acknowledges that the United States Government retains a non-exclusive, paid-up, irrevocable, world-wide license to publish or reproduce the published form of this manuscript, or allow others to do so, for United States Government purposes. The Department of Energy will provide public access to these results of federally sponsored research in accordance with the DOE Public Access Plan (https://www.energy.gov/doe-public-access-plan).

979-8-3315-8138-1

formulations of power flow constraints, bench-marked against traditional non-linear programming models. This paper aims to address these gaps through the following key contributions:

- Formulation of a multi-objective optimization model for the optimal placement and sizing of ESS in distribution networks considering three primary objectives over a 24-hour, 24-step simulation: minimizing bus voltage deviations from nominal values, and introducing a two-stage solution for the design problem: siting first, then sizing with a novel QCQP formulation.
- A comprehensive comparison of quadratic formulations, and convex formulations of power flow constraints and benchmark them with respect to the non-linear formulations in terms of ESS sizing, siting, installation cost, and objective function value.

The rest of the paper is organized as follows. Section II formally introduces the ESS placement and sizing problem as a nonconvex mixed-integer program (MIP) with non-linear constraints. Section III then introduces our novel QCQP formulation, and Section IV presents a convex relaxation. Section V details a two-step heurisitic for solving ESS placement and sizing, and then Section VI discusses simulation results and provides a comprehensive comparison of the three problem formulations. Finally, we conclude with a few avenues for further research in Section VII.

II. Design problem formulation

Consider a power network $\mathcal{N} = (\mathcal{B}, \mathcal{L})$ where $\mathcal{B}$ denotes the set of buses and $\mathcal{L}$ denotes the set of transmission lines. We assume there is electric demand, also called load, at each bus. In addition, we assume certain buses can supply power, either because they act as the network's substation, or because they are equipped with an ESS. Without loss of generality, we label the buses in $\mathcal{B}$ by $i = 1, \ldots, M$, and we label the network substation $i = 1$. The aim of the ESS Design Problem (ESSDP) is to determine the optimal placement and sizing of a number of ESS units to satisfy the power demanded at each bus while minimizing voltage fluctuations across the buses, the active power drawn from the substation, and the total installation cost of the ESS units.

A. Objective

We formulate this problem as a multi-objective program with three primary objectives. Let $P^t_{g,i}$ and $Q^t_{g,i}$ denote the real and reactive power generated at bus i during time period t; correspondingly, $P^t_{d,i}$ and $Q^t_{d,i}$ denote the real and reactive power demanded at bus i during time period t. Furthermore, let U_i denote the complex voltage at bus i, and express it in polar form as $U_i = |U_i|(\cos\theta_i + \mathrm{i}\sin\theta_i)$. Here $\mathrm{i} = \sqrt{-1}$.

We follow power system analysis conventions and normalize the voltage magnitude against the initial substation voltage and express all voltage magnitudes in per unit (p.u.). Thus the nominal value is unity.

The voltage deviation and substation power deviation objectives are given by:

$$C_V(U) = \sum_{t\in\mathcal{T}}\sum_{i\in\mathcal{B}} \left(|U^t_i| - 1\right)^2, \quad \text{and} \tag{1}$$

$$C_S(P) = \sum_{t\in\mathcal{T}} \left|P^t_{g,1} - \overline{P}\right|, \tag{2}$$

with $\overline{P}$ denoting the average substation power. We model the installation cost of the ESS at bus i as a quadratic function of the system's energy storage capacity E_i. Thus the total installation cost is given by

$$C_B(E) = \sum_{i\in\mathcal{B}} \left(a_i E_i^2 + b_i E_i + s_i c_i\right), \tag{3}$$

with $s_i \in \{0, 1\}$ denote whether bus i is equipped with an ESS. The overall objective is to minimize the linear combination:

$$\alpha C_V + \beta C_S + \gamma C_B, \tag{4}$$

for some $\alpha, \beta, \gamma > 0$.

Our multi-objective formulation reflects the complicated real-world trade-offs that arise in the deployment of ESS units to commercial networks; the problem constraints tie all the variables together, thereby creating complex Pareto fronts.

B. Constraints

For any given $s \in \{0, 1\}^M$, the network $\mathcal{N}$ models a physical transmission network, so every feasible solution to the ESSDP satisfies the constraints of an Optimal Power Flow (OPF) problem on $\mathcal{N}$ with the buses in $\{i \in \mathcal{B} \mid s_i = 1\}$ acting as generators. Thus, we begin by recalling an alternative formulation to the OPF problem in the so-called "rectangular form [15], [16]." Let G_{ij} and B_{ij} denote the conductance and susceptance of each line $(i, j) \in \mathcal{L}$. Set $G_{ii} = g_{ii} - \sum_{j\neq i} G_{ij}$ and $B_{ii} = b_{ii} - \sum_{j\neq i} B_{ij}$, with g_{ii} and b_{ii} denoting the shunt conductance and shunt susceptance at bus $i \in \mathcal{B}$. The constraint set of the OPF problem at each time period $t \in \mathcal{T} = \{1, \ldots, T\}$ is given as follows:

$$P^t_{g,i} - P^t_{d,i} = G_{ii}|U^t_i|^2 + \sum_{j\in\delta(i)} \left(G_{ij}C^t_{ij} - B_{ij}S^t_{ij}\right) \tag{5}$$

$$Q^t_{g,i} - Q^t_{d,i} = -B_{ii}|U^t_i|^2 + \sum_{j\in\delta(i)} \left(-B_{ij}C^t_{ij} - G_{ij}S^t_{ij}\right), \tag{6}$$

$$C^t_{ij} = |U^t_i||U^t_j|\cos(\theta_i - \theta_j) \quad (i, j) \in \mathcal{L},\, t \in \mathcal{T}, \tag{7}$$

$$S^t_{ij} = |U^t_i||U^t_j|\sin(\theta_i - \theta_j), \quad (i, j) \in \mathcal{L},\, t \in \mathcal{T}, \tag{8}$$

$$\underline{U_i} \le |U^t_i| \le \overline{U_i}, \qquad i \in \mathcal{B},\, t \in \mathcal{T}, \tag{9}$$

$$s_i \cdot \underline{P_{g,i}} \le P^t_{g,i} \le s_i \cdot \overline{P_{g,i}}, \qquad i > 1,\, t \in \mathcal{T}, \tag{10}$$

$$s_i \cdot \underline{Q_{g,i}} \le Q^t_{g,i} \le s_i \cdot \overline{Q_{g,i}}, \qquad i > 1,\, t \in \mathcal{T}. \tag{11}$$

Constraints (5) and (6) represent the conservation of active and reactive power flows at each bus, at each time period. Here $\delta(i)$ denotes the set of buses adjacent to bus i. Constraint (9) restricts the voltage magnitudes to be close to the initial substation voltage at all times; both $\underline{U_i}$ and $\overline{U_i}$ are close to 1 p.u. for every bus i. Constraints (10) and (11) limit the real and reactive power output by each ESS unit according to its physical capacity at every bus i for which $s_i = 1$, and they ensure no power is generated at a bus that's not equipped with an ESS, i.e., at buses for which $s_i = 0$. The trigonometric terms in constraints (7) and (8) present a formidable obstacle in the solution of large-scale OPF problem instances; the convex relaxation introduced in this work provides a workable alternative.

The ESSDP imposes several additional constraints. For starters, the total power generated is required to meet the demand at each time period. In addition, to ensure practical feasibility, we require that each ESS unit installed has enough capacity to cover peak power output over the time horizon. We consider the case where at most N ESS units can be installed.

979-8-3315-8138-1

In symbols, this means the ESSDP features the following additional constraints.

$$\sum_{i\in\mathcal{B}} P_{g,i}^t = \sum_{i\in\mathcal{B}} P_{d,i}^t, \qquad t\in\mathcal{T}, \tag{12}$$

$$E_i = \max_{t\in\mathcal{T}} |P_{g,i}^t|, \qquad i\in\mathcal{B}, \tag{13}$$

$$\sum_{i\in\mathcal{B}} s_i \le N, \tag{14}$$

$$s_1 = 0. \tag{15}$$

All in all, we obtain the non-linear non-convex ESSDP MIP:

$$\begin{aligned} &\text{minimize} \;\; (4) \\ &\text{s.t.} \quad (5)-(15). \end{aligned} \tag{16}$$

III. QCQP FORMULATION

For the sake of solver performance comparison, and as a stepping stone towards a convex relaxation, we follow [16] to define a QCQP formulation of the ESSDP that produces the optimal power outputs for Problem (16) on a radial network. The QCQP results from the change of variables defined by $C_{ii}^t = |U_i^t|^2$ together with (7) and (8). Under this change of variables, constraint (9) becomes

$$\underline{U_i}^2 \le C_{ii}^t \le \overline{U_i}^2, \qquad i\in\mathcal{B}, t\in\mathcal{T}. \tag{17}$$

Notice the new variables satisfy symmetry relations and a Pythagorean identity:

$$C_{ij}^t = C_{ji}^t, \quad S_{ij}^t = -S_{ji}^t, \qquad (i,j)\in\mathcal{L}, t\in\mathcal{T} \tag{18}$$

$$\left(C_{ij}^t\right)^2 + \left(S_{ij}^t\right)^2 = C_{ii}^t \cdot C_{jj}^t \qquad (i,j)\in\mathcal{L}, t\in\mathcal{T}. \tag{19}$$

And so the feasible set is now described by the linear and quadratic constraints (5) and (6), together with (11)–(15) and (17)–(19). Note that constraint (13) is readily enforced by the linear constraints $E_i \ge P_{g,i}^t$ and $E_i \ge -P_{g,i}^t$, for $i\in\mathcal{B}, t\in\mathcal{T}$.

To obtain a bona fide QCQP, we must produce a quadratic objective. Under the change of variables, the voltage deviation term (1) becomes

$$\sum_{t\in\mathcal{T}}\sum_{i\in\mathcal{B}} \left(\sqrt{C_{ii}^t} - 1\right)^2. \tag{20}$$

which is clearly not quadratic in the problem variables.

Our main insight here is that the voltage magnitudes are restricted to a small interval around 1 p.u., so we can leverage a Taylor expansion to recover a quadratic objective without sacrificing much accuracy. Concretely, the second-order Taylor polynomial approximating $f(x) = (\sqrt{x}-1)^2$ around $x = 1$ is $q(x) = \frac{1}{4}(x-1)^2$, and Taylor's theorem guarantees that the residual in $[1-\epsilon_-, 1+\epsilon_+]$ is bounded by $\frac{3}{4!(1-\epsilon_-)^{\frac{5}{2}}}\max\{\epsilon_-,\epsilon_+\}^3$. In the real-world power systems considered in this work, voltage magnitudes are restricted within 5% of the reference value, so $\epsilon_- = \epsilon_+ = 0.05$, and the maximum residual is less than 1.74×10^{-4}.

Thus we define the voltage deviation term in the new variables as

$$C_{V,QCQP} = \frac{1}{4}\sum_{t\in\mathcal{T}}\sum_{i\in\mathcal{B}} \left(C_{ii}^t - 1\right)^2. \tag{21}$$

Together with (2) and (3), we obtain a multi-objective QCQP formulation in the real variables C, S, E, P_g, P_d, and the binary vector s:

$$\begin{aligned} &\text{minimize} \;\; \alpha C_{V,QCQP} + \beta C_P + \gamma C_B \\ &\text{s.t.} \quad (5),\ (6),\ (11)-(15),\ (17)-(19). \end{aligned} \tag{22}$$

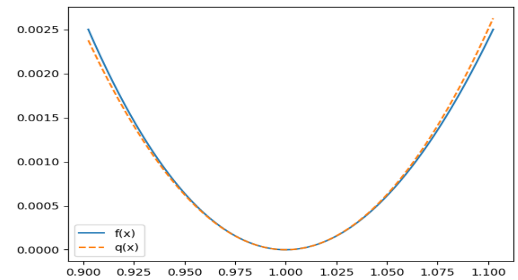

Fig. 1. The second-order Taylor approximation $q(x)$ of $f(x) = (\sqrt{x}-1)^2$ around $x = 1$ in a typical interval limiting voltage magnitude deviations of 0.05 p.u. The maximum absolute error is 1.27×10^{-4} and the root-mean-square error is 4.73×10^{-5}.

IV. CONVEX RELAXATION

While (22) is convex in the new problem variables and the feasible set of our QCQP is described by linear and quadratic constraints, the problem is not convex because the quadratic equalities (19) describe nonconvex sets.

To obtain a convex relaxation, we take a cue from [16]: we relax (19) as

$$\left(C_{ij}^t\right)^2 + \left(S_{ij}^t\right)^2 \le C_{ii}^t \cdot C_{jj}^t \qquad (i,j)\in\mathcal{L}, t\in\mathcal{T}. \tag{23}$$

Then (23) can be rewritten as

$$\left(C_{ij}^t\right)^2 + \left(S_{ij}^t\right)^2 + \left(\frac{C_{ii}^t - C_{jj}^t}{2}\right)^2 \le \left(\frac{C_{ii}^t + C_{jj}^t}{2}\right)^2,$$

which is nothing more than a rotated cone in $\mathbb{R}^4$. Note this SOCP constraint defines the convex hull of (19).

Thus relaxing (19) as (23) in our QCQP formulation yields a disciplined convex program in the real variables C, S, E, P_g, P_d, for any given s:

$$\begin{aligned} &\text{minimize} \;\; \alpha C_{V,QCQP} + \beta C_P + \gamma C_B \\ &\text{s.t.} \quad (5),\ (6),\ (11)-(15),\ (17)-(18),\ (23). \end{aligned} \tag{24}$$

V. TWO-STAGE SOLUTION OF THE MIXED-INTEGER PROGRAM

The ESSDP is a MIP because the ESS placement variables s_i are binary. We propose a two-stage heuristic. First, the placement of ESS across the network is determined by formulating the siting problem as follows where the first constraints indicates that the summation of energy storage capacity should satisfy the total load:

$$\begin{aligned} \text{minimize} \;\; & \sum_{i\in\mathcal{B}} s_i C_i(E_i) \\ \text{s.t.} \;\; & \sum_{i\in\mathcal{B}} s_i \overline{E_i} \ge \sum_{i\in\mathcal{B}} P_{d,i} \\ & \sum_{i\in\mathcal{B}} s_i \le N. \end{aligned} \tag{25}$$

In this stage, the decision is based on the total cost of ESS installation, and the energy capacity. Importantly, the siting problem does not explicitly account for voltage deviation or substation power deviation; rather, it focuses on the economic aspect of deployment. Here, the total number of binary states per ESS unit is 2 (present or not present). If the number of buses of a network is M, there will be M option to site the ESS and the number of binary states will be 2^M. So, the number of binary states will increase exponentially with number of buses. This problem is solved through a quadratic programming approach.

Second, with ESS locations (s_i) in hand, the sizing problem is solved using the optimization problem formulation in

979-8-3315-8138-1

Sections II, III, and IV. The sizing stage incorporates voltage deviation minimization, substation power deviation reduction, and the total cost of ESS in determined bus positions into the objective function. For each candidate location, the optimal real power requirement is determined for every time interval, and the optimal storage capacity of each ESS results from the peak power requirements.

VI. Simulations and Result Analysis

To validate the proposed methodology, both the siting and sizing problems were solved using a classical mixed-integer optimization framework and applied to the two standard test cases. The test cases are: Test Case I: 12-bus distribution system, and Test Case II: 32-bus distribution system.

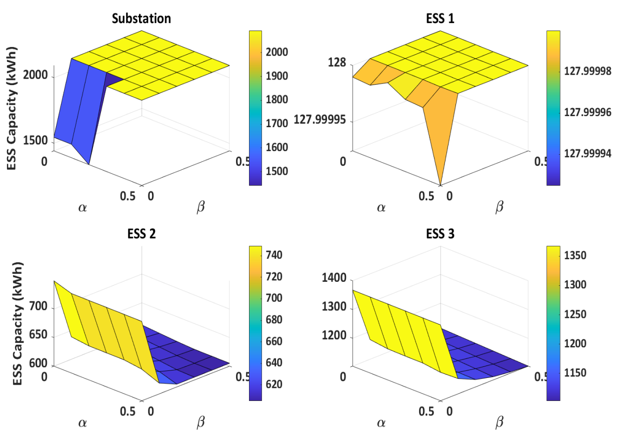

Fig. 2. Sensitivity analysis of Test Case I for different values of α, and β for non-linear formulation (for scaling simplicity, α, and β is normalized by 100, and 10, respectively.

For, both cases, the average bus voltage ($\overline{U}$), sub-station voltage, and the average substation power ($\overline{P}$) were considered as 1.0 p.u., 1.0 p.u., and 0.5 MW, respectively. The installation costs were assumed to be identical across all possible locations, and the cost function C_i is considered as $\{a, b, c\} = \{0.01, 460, 1\}$ for a quadratic function, $C_i = ax^2 + bx + c$ [17]. The 24-hour load profile is taken from the EPRI US load factor {0.677, 0.6256, 0.6087, 0.5833, 0.58028, 0.6025, 0.657, 0.7477, 0.832, 0.88, 0.94, 0.989, 0.985, 0.98, 0.9898, 0.999, 1, 0.958, 0.936, 0.913, 0.876, 0.876, 0.828, 0.756} [18].

A. Test Case I: 12-Bus Distribution System

The 12-bus distribution system is derived from the IEEE 13-bus distribution system. For clarity in presentation, the original bus numbering of the IEEE 13-bus system was renumbered and bus-680 is removed. A single-phase equivalent representation of the multi-phase IEEE 13 bus system was considered for the evaluation of the solution methods proposed in this paper. The system's data are taken from [19]. In the modified system, the switch between bus-671 and bus-692 was assumed to be closed. All network parameters were converted into the per-unit (p.u.) system for consistency. The on-load tap changer (OLTC) transformer located between bus-650 and bus-632 was modeled with a fixed tap position of 0 throughout the study.

Fig. 3 illustrates the voltage profile of the 12-bus distribution system under the specified operating conditions for (a) non-linear constraints, (b) quadratic constraints, and (c) convex constraints. It can be observed that the bus voltages vary between 0.95 p.u. - 1.045 p.u. for all the three formulations. The lowest voltages occur around bus-675 (bus-12 in Fig. 3) for all the three formulations. In contrast, bus-652, and bus-611

TABLE I
Sub-station max. real power, ESS capacity for one hour, $C_V(U)$, and Objective function value (unit) for Test Case-I

Description	Non-linear	Quadratic	Convex
Sub-station Ps (kW)	2092	2093	500
ESS Capacity (kWh)	128	128	823.0
	607.4	607.4	1660.3
	1117.7	1116.7	607.3
$C_V(U)$	8.73	9.31	0.25
Obj. function	476.7	477.5	461.6

(bus-9, and bus-10 in Fig. 3) exhibit higher voltage magnitudes, reaching values 1.045 p.u. This over voltage trend is due to the position of the capacitor bank on bus-611. It is worth mentioned that the 12 buses are numbered from 0 to 11 in Fig. 3

The optimal ESS position is determined as the bus 634, 652, and 611 (bus 6, 9, and 10). In comparison, a mixed integer programming solution is obtained without the separation of siting problem. In that case, all bus requires an ESS with smaller values which is not practical. With the proposed relaxation approaches, the real power from the sub-station, the ESS capacity for one hour, total voltage deviation, and objective function value are illustrated in Table I. The Non-linear model and quadratic model deliver identical substation power (2092 and 2093 kW), while the Convex model results in lower values (500.0 kW), indicating more efficient grid utilization. Across three ESS sizing scenarios, the Convex model consistently provides higher capacities, maximum being at 1660.3 kWh, followed by Quadratic and Non-linear models. In terms of objective function values, the Convex formulation incurs the lowest expense (461.6 units). The time of convergence (ToC) for the non-linear and quadratic models are 5.77, and 7.13 seconds, respectively. In addition, the convex model has the lowest total voltage deviation of 0.25. The sensitivity analysis is performed for all the models by changing the value of α, β, and γ and the non-linear model is illustrated in Fig. 2, which shows that most optimal solution comes when the values of $\alpha \approx 33$, $\beta \approx 3.3$, and $\gamma \approx 0.33$.

B. Test Case II: 32-Bus Distribution System

We tested the methods with 32-bus distribution system, which is a modified version of IEEE-33 bus distribution system. The system data are taken from [20]. The voltage rating of the system is 12.66 kV and comprising of 31 branches. The total load of the system is 3.715 MW and 2.8 Mvar. Fig. 4 illustrates the 24-hour voltage profiles across a 32-bus distribution. The voltage profiles show that the convex model maintains the most stable and tightly regulated voltage levels across all buses, consistently staying within the range of 0.985 to 1.01 p.u. In contrast, the non-linear, and quadratic formulations illustrate more fluctuations.

The optimal ESS position is determined as the bus 12, 24, 25, and 26. Table II presents a comparative evaluation of Non-linear, Quadratic, and Convex optimization formulations applied to Test Case-II. The Non-linear model provides the highest substation power output at 842.9 kW, while the quadratic model achieves the lowest at 604.1 kW. In terms of objective function value, the three models incur expense as 472.5, 594.3, and 492.1 units, respectively. In addition, like in Test Case I, the total voltage deviation of the convex model is lowest at 2.24. The ToC for the non-linear and quadratic models are 22.17, and 16.91 seconds, respectively.

VII. Conclusion and Future Work

In this paper, the formulations of multi-objective two-stage optimization framework for the siting and sizing of ESS in

979-8-3315-8138-1

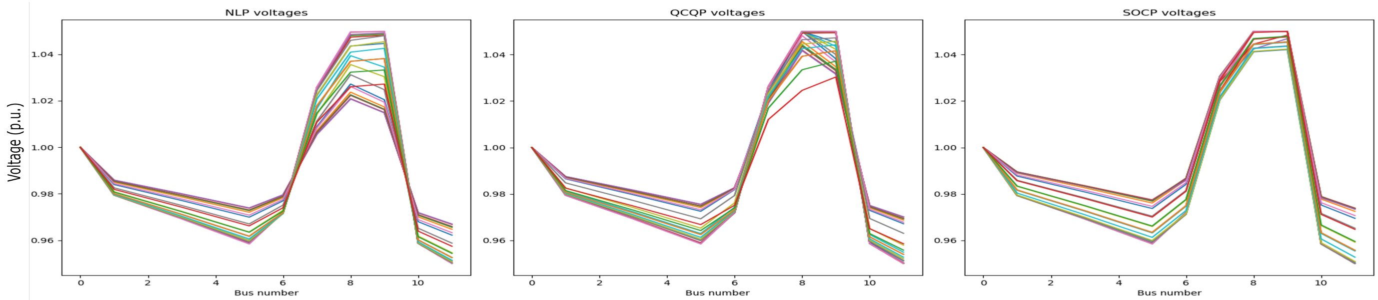

Fig. 3. Voltage profiles over 24 hours for the IEEE 12-bus distribution system obtained by solving the non-linear problem (16) (left), our QCQP formulation (22) (center), and our convex relaxation (24) (right).

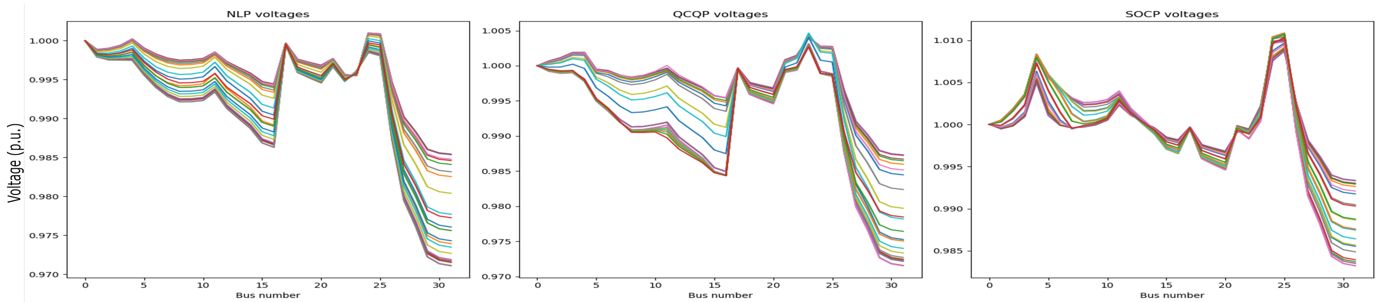

Fig. 4. Voltage profiles over 24 hours for the IEEE 32-bus distribution system obtained by solving the non-linear problem (16) (left), our QCQP formulation (22) (center), and our convex relaxation (24) (right).

TABLE II
SUB-STATION MAX. REAL POWER, ESS CAPACITY FOR ONE HOUR, $C_V(U)$, AND OBJECTIVE FUNCTION VALUE (UNIT) FOR TEST CASE-II

Description	Non-linear	Quadratic	Convex
Sub-station Ps (kW)	842.9	604.1	640.3
ESS Capacity (kWh)	604.4	735	999.9
	645.1	1000	1000
	822.2	1000	110
	830.9	1000	1000
$C_V(U)$	2.32	2.41	2.24
Obj. function	472.5	594.3	492.1

distribution networks with non-linear, quadratic and convex formulations addressing key operational goals such as minimizing voltage deviation, reducing substation average real power flow, and lowering installation costs for a 24-hours 24-steps simulations are discussed. A comprehensive comparison of these three formulations for determination of ESS sizing and siting of two test cases are provided. From the optimization results, it is evident that formulations with convex relaxations shows less total voltage deviation for both cases which will be very effective for large scale non-linear mixed integer optimization (MIO) problem. Furthermore, the MIO problem formulated in this work is segregated into two stage binary and classical optimization problem.

The presented MIO problem formulations coupled with the comparison study provides a concrete evidence that the optimization problem formulated with convex relaxation can be a good fit for evaluating feasibility of emerging quantum-classical hybrid optimization approaches. In the future, these formulations will form the stepping stone for solving large-scale mixed integer optimization problems, which are highly non-linear, and complex on quantum computers.

REFERENCES

[1] M. S. Hasan et al., “Centralized volt-var-watt optimization for real distribution grids,” in *2024 IEEE Power Energy Society General Meeting (PESGM)*, 2024.

[2] T. Jaradat and T. Khatib, “Optimal sizing of battery energy storage system in electrical power distribution network,” *Energy Exploration & Exploitation*, vol. 43, no. 3, pp. 909–931, 2025.

[3] K. Wichitkrailat et al., “Optimal sizing and locations of multiple besss in distribution systems using crayfish optimization algorithm,” *IEEE Access*, vol. 12, pp. 94 733–94 752, 2024.

[4] M. B. Hossain et al., “Advancement of fuel cells and electrolyzers technologies and their applications to renewable-rich power grids,” *Journal of Energy Storage*, vol. 62, p. 106842, 2023.

[5] B. Li et al., “Review on photovoltaic with battery energy storage system for power supply to buildings: Challenges and opportunities,” *Journal of Energy Storage*, vol. 61, p. 106763, 2023.

[6] H. Masrur et al., “Cost-aware modeling and operation of interconnected multi-energy microgrids considering environmental and resilience impact,” *Applied Energy*, vol. 356, p. 122320, 2024.

[7] J. An and T. Hong, “Multi-objective optimization for optimal placement of shared battery energy storage systems in urban energy communities,” *Sustainable Cities and Society*, vol. 120, p. 106178, 2025.

[8] H. Nazaripouya et al., “Optimal sizing and placement of battery energy storage in distribution system based on solar size for voltage regulation,” in *2015 IEEE Power & Energy Society General Meeting*.

[9] M. Zolfaghari et al., “Optimal sizing of battery energy storage systems in off-grid micro grids using convex optimization,” *Journal of Energy Storage*, vol. 23, pp. 44–56, 2019.

[10] B. Khaki, “Joint sizing and placement of battery energy storage systems and wind turbines considering reactive power support of the system,” *Journal of Energy Storage*, vol. 35, p. 102264, 2021.

[11] H. I. Alhammad et al., “Capacity optimization and optimal placement of battery energy storage system for solar pv integrated power network,” in *2021 IEEE Energy Conversion Congress and Exposition (ECCE)*. IEEE, 2021, pp. 847–852.

[12] J. Wang et al., “Multi-objective optimal allocation of battery energy 3storage systems in distribution network with high penetration of renewable energy,” in *2025 IEEE 3rd International Conference on Power Science and Technology (ICPST)*, 2025, pp. 1281–1287.

[13] M. Yang et al., “Optimal placement and configuration of hybrid energy storage system in power distribution networks with distributed photovoltaic sources,” in *2018 2nd IEEE Conference on Energy Internet and Energy System Integration (EI2)*. IEEE, 2018, pp. 1–6.

[14] G. Optimization, “4 key advantages of mov’s heuristics,” *Mathematical Optimization vs. Heuristics*, pp. 1–7, 2022.

[15] R. Jabr, “Radial distribution load flow using conic programming,” *IEEE Transactions on Power Systems*, vol. 21, no. 3, pp. 1458–1459, 2006.

[16] B. Kocuk et al., “Strong SOCP relaxations for the optimal power flow problem,” *Operations Research*, vol. 64, no. 6, pp. 1177–1196, 2016.

[17] C. K. Das et al., “Optimal placement of distributed energy storage systems in distribution networks using artificial bee colony algorithm,” *Applied energy*, vol. 232, pp. 212–228, 2018.

[18] D. Montenegro and R. Dugan, “Opendss and opendss-pm open source libraries for ni labview,” in *2017 IEEE Workshop on Power Electronics and Power Quality Applications (PEPQA)*. IEEE, 2017, pp. 1–5.

[19] K. P. Schneider et al., “Analytic considerations and design basis for the ieee distribution test feeders,” *IEEE Transactions on Power Systems*, vol. 33, no. 3, pp. 3181–3188, 2018.

[20] M. S. Hasan et al., “Semi-definite programming based scalable and accurate optimal power flow models for radial distribution networks,” *IEEE Transactions on Industry Applications*, vol. 60, no. 1, pp. 1463–1475, 2024.

979-8-3315-8138-1